1997 Kronotsky earthquake and tsunami and their predecessors, Kamchatka, Russia

Joanne Bourgeois[1], Tatiana K. Pinegina[2]

[1]Department of Earth and Space Sciences, University of Washington, Seattle, WA 98195-1310, USA
[2]Institute of Volcanology and Seismology, FEB RAS, 9 Piip Boulevard, Petropavlovsk-Kamchatsky, 683006, Russia

Correspondence to: Joanne Bourgeois (jbourgeo@uw.edu)

Abstract. The northern part of the Kamchatka subduction zone (KSZ) experienced three tsunamigenic earthquakes in the 20th century -- Feb 1923, April 1923, Dec 1997 -- events that help us better understand the behavior of this segment. A particular focus of this study is the nature and location of the 5 December 1997 Kronotsky rupture (Mw ~7.8) as elucidated by tsunami runup north of Kronotsky Peninsula in southern to central Kamchatsky Bay, Some studies have characterized the subduction zone off Kronotsky Peninsula as either more locked or more smoothly slipping than surrounding areas and have placed the 1997 rupture south of this promontory. However, 1997 tsunami runup north of the peninsula, as evidenced by our mapping of tsunami deposits, requires the rupture to extend farther north. Previously reported runup (1997 tsunami) on Kronotsky Peninsula was no more than 2-3 m, but our studies indicate tsunami heights for at least 50 km north of Kronotsky Peninsula in Kamchatsky Bay, ranging from 3.4 to 9.5 m (average 6.1 m), exceeding beach ridge heights of 5.3 to 8.3 m (average 7.1 m). For the two 1923 tsunamis, we cannot distinguish their deposits in southern to central Kamchatsky Bay, but the deposits are more extensive than the 1997 deposit. A reevaluation of the April 1923 historical tsunami suggests that its moment magnitude could be revised upward, and that the 1997 earthquake filled a gap between the two 1923 earthquake ruptures. Characterizing these historical earthquakes and tsunamis in turn contributes to interpreting the prehistoric record, which is necessary to evaluate recurrence intervals for such events. Deeper in time, the prehistoric record back to ~300 A.D. in southern to central Kamchatsky Bay indicates that during this interval, there were no local events significantly larger than those of the 20th century. Together, the historic and prehistoric tsunami record suggests a more northerly location of the 1997 rupture compared to most other analyses, a revision of the size of the April 1923 earthquake, and agreement with previous work suggesting the northern KSZ ruptures in smaller sections than the southern KSZ. The latter conclusion requires caution, however, as we continue to learn that our historic and even prehistoric records of earthquakes and tsunamis are limited, in particular as applied to hazard analysis. This study is a contribution to our continued efforts to understand tectonic behavior around the northern Pacific and in subduction zones, in general.

1 Introduction

In this paper we intend to illustrate how tsunamis may inform interpretations of their earthquake sources. For example, by presenting previously unpublished tsunami-deposit data we show that the December 1997 Kamchatka tsunami requires a different earthquake source region than geophysically interpreted, a source that lies between prior historical events (in a seismic gap). This conclusion leads us to the question, Do earthquakes in the northern part of the Kamchatka Subduction Zone (KSZ) characterize it as rupturing in shorter segments than the southern part? We address this question, particularly for northern portion, by studying the history and the prehistory of tsunamis in this region. In conducting this analysis, we illustrate some of the strengths and limitations of reconstructing prehistoric tsunamis, even with strong age control from well-dated and well-mapped tephra.

Without post-tsunami or tsunami-deposit surveys, remote spots in the world may experience large events without a written record, as illustrated, e.g., by references to the "modest" or "small" tsunami of the 15 December 2006 central Kurils earthquake (Ammon et al., 2008; Liu, 2009). In fact this tsunami generated an average of 9.6 m runup over an along-rupture length of 390 km (MacInnes et al., 2009). The case we present herein of the 5 December 1997 tsunami following the Mw 7.7-7.9 Kronotsky earthquake (Fig. 1, Fig. 2), however, is even more complex historically, because there *was* a post-tsunami survey quickly following (Zayakin and Pinegina, 1998), though of limited extent. The local tide-gage record for this 1997 tsunami is also incomplete, and deep-water pressure recorders deployed at the time were not positioned to get distinctive recordings from a tsunami originating near Kronotsky Cape (Bourgeois and Titov, 2001). The earthquake and tsunami occurred in the dark of a December night in an area with no permanent settlements.

In the summer of 2000, we conducted a field survey for historical and paleo- tsunami deposits in south Kamchatsky Bay (Fig. 1), north of Kronotsky Peninsula. We expected to find evidence for historical Kamchatka tsunamis such as 1923 (Table 1; Table S1), but not for 1997 Kronotsky because on the Kronotsky Peninsula, the post-tsunami survey found evidence of quite limited runup. Thus we were surprised to find a sand layer just at the surface, covered only by plant debris such as grass and leaves, distributed much as we have come to expect of tsunami deposits, and at elevations of 5 m or more above sea level. Although we were skeptical at first, we could find no alternative to explain the layer and its distribution other than a tsunami from the 1997 earthquake.

The implications of this case, where an earthquake was analyzed without full knowledge of its tsunami, are several. First, the fact that there was runup greater than that reported by a post-tsunami survey changes our view of the tsunami as well as of the earthquake. Further, the size of the tsunami, based on its deposits and a corroborating eyewitness account (acquired in 2001), helps constrain rupture characteristics of this earthquake. This constraint in turn leads to an interpretation of segmentation of the northern KSZ, and our interpretation that the tsunamigenic portion of this earthquake rupture occurred in a gap between two 1923 tsunamigenic earthquakes.

This recent historical tsunami also helps us interpret earlier historical and well as prehistoric earthquakes and tsunamis along the northernmost part of the Kuril-Kamchatka subduction zone. Tsunamis originating from this region commonly have an impact not only locally but also on Hawaii, as did the February 1923 tsunami, and in some cases even on the western coast of the Americas, as did the 2006 central Kurils tsunami.

72 **2 Background**

73 **2.1 The 1997 Kronotsky earthquake**

74   On 5 December 1997 at 23:26:51 local time (11:26:51 UTC), a large earthquake (Mw 7.7-7.9; we use 7.8)

75 shook the region of the Kronotsky Peninsula, Kamchatka, Russia (Fig. 1, Fig. 2; Gordeev et al., 1998). The

76 earthquake was characterized by a typical foreshock-mainshock-aftershock sequence (Gusev et al., 1998; Fedotov et

77 al., 1998; Balakina, 2000; Zobin and Levina, 2001; Kuzin et al. 2007; Slavina et al., 2007). Most studies of the

78 earthquake calculate a moment magnitude of 7.8 for the energy released in the first 60-80 seconds of the main

79 rupture (e.g., Zobin and Levina, 2001). Gusev and Shumilina (2004), in reassessing many Kamchatka earthquakes,

80 assign Mw 7.9 to Kronotsky 1997. In addition to the mainshock, and using GPS measurements, Gordeev et al.

81 (2001) calculate Mw 7.7 for deformation in the *pre-seismic* half month, and approximately Mw 7.9 for *post-seismic*

82 deformation; Bürgmann et al. (2001) calculate Mw 7.7 of (*post-seismic*) aseismic energy release in the 2 months

83 following the mainshock, also based on GPS data.

84   The locations of the mainshock and of any slip concentration for this earthquake have not been well

85 resolved, and with one early exception (Sohn, 1998), locators have not used tsunami data. Based on seismic data, the

86 locations of foreshocks and the mainshock/epicenter (Fig. 2) are in the northern part of the interpreted rupture area.

87 A number of analytical locations of the mainshock lie under the NE Kronotsky Peninsula (Fig. 2; Table S2). Some

88 analyses interpret the rupture to have propagated NE to SW (Petukhin et al., 1998), deepening toward the SW.

89 Gusev (2004) maps the entire aftershock zone as part of the 1997 event (Fig. 1). On the other hand, the linear zone

90 of aftershocks in the SW (Fig. 2) has been interpreted to be a separate stress zone (Kuzin et al., 2007) potentially

91 along a separate transverse fault (Slavina et al., 2007). In an analysis focused on GPS data, Bürgmann et al. (2001)

92 place the majority of the primary rupture energy in the southern half of the aftershock zone.

93

94 **2.2 The recorded 1997 Kronotsky tsunami**

95   The most complete contemporary record of the 1997 Kronotsky tsunami is from far-field tide gages. Both

96 proximal tide gages, in Ust' Kamchatsk and in Nikolskoe (Bering Island) (Fig. 1), were not functioning when the

97 tsunami arrived. The Petropavlovsk-Kamchatsky gage is very protected and shows a wave train with an amplitude

98 of about 0.01 m (Zayakin and Pinegina, 1998). The tide gage at Nikolskoye resumed recording after the first 10

99 hours of the tsunami, with a few cm of amplitude remaining (Zayakin and Pinegina, 1998). The far-field tsunami

100 had tide-gage amplitudes in Alaska/Aleutians and Hawaii in line with other tsunamis traveling to Hawaii from the

101 Russian Far East (Table S3; Fig. S4). The tsunami was recorded on at least 12 tide gages, with the highest amplitude

102 (half of wave height) of 0.3 m at Kahului, Maui, Hawaii (NCEI online database). Deep-water pressure sensors

103 deployed at that time in the north Pacific were all in tsunami shadows for this tsunami source, and in all cases, the

104 modeled and measured tsunami was within the noise level of the buoys (Bourgeois and Titov, 2001; no event page

105 at http://nctr.pmel.noaa.gov/database_devel.html).

106   A truncated post-earthquake and tsunami survey by helicopter took place on 9 December 1997 (Leonov,

107 1998; Zayakin and Pinegina, 1998). The survey reached as far north as Kronotsky Cape on the Kronotsky Peninsula

108 (Fig. 1) and found that the tsunami had not exceeded the unvegetated sandy beach. At this time, the beach was

109 covered with a thin layer of ice and snow, which in places had been coated by the tsunami with a thin sand layer and
110 elsewhere had been broken up by the tsunami (Fig. 3). The team did not have surveying equipment and estimated
111 runup to be no more than 3 m (T. Pinegina notes), and the published report gave a maximum of 1-1.5 m. The
112 turnaround point in the survey was dictated by fuel and available daylight.
113   On 5 December 1997, two rangers were in a cabin near Big Chazhma River (Fig. 1); one of them was
114 interviewed (in Petropavlovsk-Kamchatsky) by T. Pinegina 19 April 2001. They felt the earthquake that night, and
115 the next day, as was their custom, they went via snowmobile to survey the northern coastal part of Kronotsky
116 reserve, to the Little Chazhma River area. At the mouth of the Big Chazhma, they saw jumbled ice and seaweed on
117 the snow; a cabin on the south bank of the Little Chazhma River was partly wetted, and there was seaweed on the
118 snow. Normally the rangers crossed the river near this cabin, but the river was a jumble of ice and they had to go
119 some distance upstream in order to cross (on ice). On the other side, they could not continue north because there was
120 water in the low spot between beach and hill (see Fig. 4, our profile 100).
121   Based on results of the post-tsunami survey (reported to Sohn by V. Gusiakov), Sohn (1998) analyzed the
122 tsunami with regard to its earthquake source and concluded that the main rupture must have lain largely under land,
123 in order to explain the low runup accompanying a moment magnitude she calculated as Mw 7.7.
124
125 **2.3 Historical record of earthquakes and tsunamis affecting the field area**
126   The Kamchatka Peninsula has a short but rich historic record of large earthquakes and attendant tsunamis,
127 of which we discuss herein only 20th century tsunamis originating in or having been recorded in the field region of
128 Kamchatsky Bay (Table 1). In addition to locally originated tsunamis, Kamchatka is vulnerable to tsunamis from
129 Chile, less so from Peru, and not so much from Japan, Alaska, Aleutians and Central America, due to directivity
130 (e.g., see Table S1). Based on scant records (Table 1), the 1960 Chile tsunami likely reached elevations of 3-5 m
131 above sea level along Kamchatsky Bay (Fig. 1), on the order of twice as high as the 1952 southern Kamchatka
132 tsunami in this bay (Table 1)

133   The largest documented local tsunamis from earthquakes near Kronotsky Peninsula (Fig. 1; Table 1) are
134 two from 1923, both having local as well as farfield records (Table S4); both may have affected south-central
135 Kamchatsky Bay. There was also a 24 Feb 1923 Mw 7.6 earthquake in this area (Fig. 1; Gusev, 2004); however, it
136 has no historical tsunami record in the near or far field. The Mw 8.0 1917 earthquake along the Steller fracture zone
137 (Fig. S1) also did not produce a recorded tsunami. The 3 Feb 1923 Kronotsky Bay earthquake (Mw 8.5) was located
138 south of Kronotsky Cape (Fig. 1), and its tsunami was large (6-8 m) in Kronotsky Bay (Table 1), decreasing
139 northward; a sled team in the area during and after the earthquake reported a coastal ice rampart being pushed about
140 3 km upstream on the (Big?) Chazhma River, north of Kronotsky Cape. The 13 April 1923 north Kamchatsky Bay
141 earthquake (Mw 7.3 in NCEI catalogue; 14 April local time) generated a very high tsunami in north to north-central
142 Kamchatsky Bay (Table 1; Table S1), with large(st) ("naibolshii") effects south to Cape Shubert in south-central
143 Kamchatsky Bay (Fig. 1) (Troshin and Diaghilev, 1926). [Based on tsunami amplitudes, Gusev and Shumilina
144 (2004) suggested this April 1923 earthquake had a moment magnitude of 8.2 (Table S1, Fig. S2).] In sum, the

145 February and April tsunami runup was large south and north (respectively) of our field area, decreasing toward that

146 field area.

147 The record of earthquakes and tsunamis on Kamchatka prior to the 20th century is spotty but improving

148 (Zayakin and Luchinina, 1987; Godzikovskaya, 2010). Earthquakes on 17 May 1841 and 17 October 1737

149 originated in the region of the 1952 south Kamchatka great earthquake, so likely did not have significant effects in

150 (southern) Kamchatsky Bay (see Table 1, 1952 runup). Other tsunamis that may have affected southern Kamchatsky

151 Bay are an autumn 1849 tsunamigenic earthquake in the vicinity of the Komandorsky Islands (Godzikovskaya,

152 2010) and a 1791 event which has an intriguing account of having affected the mouth of the Kamchatka River (Ust'

153 Kamchatsk), reported to reach 7 km upstream (Zayakin and Luchinina, 1987).

154

155 **3 Methods**

156 We measured 15 topographic profiles (Fig. 4) perpendicular to the shoreline along the coast of southern to central

157 Kamchatsky Bay (Fig. 1; Fig. S2), and made 117 hand-dug excavations along these profiles in order to document

158 historical and paleotsunami deposits. We used a surveying rod with a transit level (hand level and tape for profile

159 001 and upper part of profile 120) (methods as in Bourgeois et al., 2006). We usually excavated to 0.5-1 m deeper

160 than the lowest preserved tephra overlying clean sand (not exhibiting soil weathering).

161 It is well-established that tsunamis create sedimentary deposits as they flood a coastal plain with turbulent,

162 turbid water, and there are means to distinguish tsunami deposits from those of floods, storms and wind. The general

163 characterization of a tsunami deposit in sandy coastal systems is a sand sheet which typically thins and fines

164 landward, following topography and commonly thickening in swales (Bourgeois, 2009). Many factors, from

165 sediment availability to coastal topography and surface roughness to the velocity profile of incoming and outgoing

166 waves, play a role in sedimentation. Kamchatka field sites are primarily sandy, vegetated coastal plains and

167 associated peat marshes, where shoreline availability of sand and onshore vegetative cover maximize the likelihood

168 of generating and preserving tsunami deposits. (Many historical Kamchatka tsunamis have occurred during winter

169 snow cover; deposits would have been "let down" onto a vegetative mat as the snow melted.) In these settings, river

170 flood deposits are muddy (not clean sand), and eolian deposits are rare, not sheetlike, and consistently fine-grained;

171 storm waves and storm surge at these latitudes rarely exceed elevations and particularly distances of our surveyed

172 profiles (see Bourgeois et al., 2006).

173 We use three measurements to characterize tsunamis via their deposits (Fig. 5): sediment inundation (L),

174 sediment runup (h), and maximum height seaward of a deposit on a given profile (H). The maximum distance inland

175 of a tsunami deposit (*sediment inundation*, Fig. 5) and the deposit's elevation at sediment inundation (*sediment*

176 *runup*, Fig. 5) represent minimum estimates of tsunami extent for several reasons: Tsunami deposits can only be

177 more limited (not more extensive) than water runup and inundation, the final limit of a deposit is not always located

178 in the field on any given profile, and thin deposits may not be identified or preserved.

179 Primary age control in excavations is provided by dated regional and local marker tephra layers (Table 2),

180 which in general have been well studied on Kamchatka (e.g., Braitseva et al., 1997), although tephra in the southern

181 Kamchatsky Bay area had not previously been examined. Based on our own and previous work, as well as on more

182 recently published isopach maps (Kyle et al., 2011; Ponomareva et al., 2017), the three most consistently present

183 layers in the sections are $KSht_3$ (A.D. 1907 — we use KS_{1907})—most useful for studying the historical record, SH_{1450}

184 (A.D. ~600) and KS_1 (A.D. ~300), the latter used as the lower boundary for our tsunami statistics. A fourth marker,

185 SH_2 (A.D. ~1130), is commonly present in more northerly profiles, Recent work around Shiveluch volcano and

186 Kamchatsky Peninsula (Fig. 1) has led to redesignation of Shiveluch tephras and to more definitive model ages of

187 these tephra (Ponomareva et al., 2017). In addition to the silicic marker tephra (Table 2), there are local basaltic-

188 andesitic tephra layers, which can be from Kliuchevskoi, Bezymianniy, Tolbachik or Gamchen volcanoes; we used

189 these tephra only as local field guides. In the northernmost of our profiles, a historic ash from Bezymianniy 1955

190 (year before the 1956 paroxysmal eruption) is locally present and used as a factor in distinguishing Chile 1960

191 tsunami deposits from Kamchatka 1952.

192   For the prehistoric record of tsunami runup and inundation, topographic profiles would not necessarily be

193 the same as in the recent past and thus must be reconstructed to account for succeeding topographic changes in

194 elevation and distance along the profile. While we cannot typically reconstruct profiles that have been changed by

195 erosion, we can reconstruct profile progradation (building seaward), which affects profile width. Our method uses

196 preserved tephra as discussed, e.g., in Pinegina et al. (2013) and MacInnes et al. (2016), as summarized in Fig. S5.

197 Changes in elevation relative to sea level are quantified by determining the age and elevation of the lowest former

198 soil horizon above marine sand in any excavation (Fig. S5) (as in Pinegina et al., 2013). For the case herein,

199 reconstructing less than 2000 years of coastal history, our calculated changes in relative sea level are due to active

200 tectonics, not eustatic or regional sea-level fluctuation.

201

202 **3.1 Field localities**

203   The southern field site (Fig. 1) which we call "Chazhma" (Fig. 4) is a narrow strip (~400 m wide or less) of

204 Holocene accumulative coastline along a rugged coast just north of the Kronotsky Peninsula. The two profiles near

205 river mouths (Chazhma 210 and Chazhma 130; Fig. 4) maintain lower elevations (< 4 m) over much of their

206 distance, though both reach elevations of more than 6 m above sea level. The other five profiles rise, typically in

207 sharp steps indicative of Holocene uplift events (as in Pinegina et al., 2013), reaching typical maximum levels of 8-

208 10 m (Fig. 4). Net uplift on these profiles is consistent with longer-term uplift of Pleistocene terraces on the

209 Kronotsky Peninsula (Melekestsev et al., 1974).

210   The northern field site which we call "Storozh," extending north to the Bistraya River (Fig. 1; Fig. 4), is a

211 broader strip (typically 600 m wide) of Holocene accumulative coastal plain associated with active and drowned

212 river mouths. Two of these profiles (140, 001; Fig. 4) drop in elevation behind one or more beach ridges. The other

213 seven profiles are typified by a series of beach ridges, of which the seaward ridges are higher, reaching typically 6-7

214 m, with an average elevation of the profile in the range of 4-6 m (Fig. 4). Such profiles indicate minor subsidence or

215 no vertical change in the late Holocene.

216

217 **4 Results -- 20th century tsunami deposits**

218   In field season A.D. 2000, the sand we interpret to have been deposited by the 1997 Kronotsky tsunami

219   formed a sheet-like layer at the surface, buried only by grass, leaves and other dead vegetation, in general decreasing

220   landward in thickness and grain size. The deposit we interpret to be "1923" (from one or both of two tsunamis in

221   1923) lies above the marker tephra KS_{1907} with less soil thickness between KS_{1907} and "1923" than between the top

222   of "1923" and the base of the modern turf. Our interpretation of "1923" as well as a rare sand layer between "1923"

223   and 1997, which we assign to the 1960 Chile tsunami, is discussed below.

224   Using identified and mapped tsunami deposits, we calculate minimum sediment runup and inundation on

225   each of the 15 profiles (Table 3, Figure 6), correcting to high tide from tide at the time of survey. The 1997 tsunami

226   occurred just after high tide; in all cases, using a high tide datum gives us minimum runup values. We determine

227   minimum sediment runup (h) by the presence or absence of distinct 1997 and "1923" deposits on each profile. We

228   distinguish between profiles where the farthest landward excavation still contains the 1997 or "1923" deposit and

229   ones that do not. If no deposit is present in one or more excavations landward of ones with a deposit, the limit of

230   sediment inundation (L) occurs within the measured profile (Fig. 5, example of 1997) and actual tsunami runup is

231   estimated from sediment runup. For profiles where a particular tsunami deposit extends beyond all excavations (Fig.

232   5, example of 1923), the actual size of the tsunami could be, in some cases, significantly greater than our sediment-

233   runup and inundation minima. We also report the maximum height the tsunami had to exceed (H) as it traveled

234   along a profile (across the accumulative marine terrace). In a few cases, the farthest inland excavation was at a low

235   elevation that could have been reached via the river rather than over the profile (Table 3, Fig. 6), although the

236   deposits observed were not muddy. Note that maximum elevations and inundation distances are affected by

237   elevations and distances along actual profiles (Fig. 4), e.g., a profile cannot record sediment runup higher than its

238   maximum elevation, and a short, steep profile will record shorter sediment inundation distances.

239

240   **4.1 1997 tsunami**

241   Sediment runup data (Table 3, Fig. 6) indicate that in southern to central Kamchatsky Bay, the 1997 Kronotsky

242   tsunami ran up to as much as 9.5 m, averaging 6.1 m, with moderate inundation distances of 100-300 m. The general

243   pattern over about 100 km of coastline, including post-tsunami survey observations on Kronotsky Peninsula itself, is

244   relatively smooth, and we also expect based on the pattern that there was runup north of our northernmost profile

245   (Fig. 6), but north-central Kamchatsky Bay comprises sea cliffs, not coastal plain. The maximum elevation reached

246   by the tsunami deposit is higher on southern (Chazhma) profiles. However, lower runup numbers on northern

247   profiles may be an artefact of their lower elevations (Figure 4); inundation distances are greater on these profiles

248   (Table 3). On some profiles the 1997 deposit is absent.

249

250   **4.2 1923 tsunamis**

251   Sediment runup and inundation data for "1923" indicate that this tsunami was larger than 1997 in the region of our

252   profiles. The deposit we interpret as from 1923 is usually thicker and more extensive, and never less extensive, than

253   the deposit from 1997 (e.g., Figs. 5,7,8,9). The "1923" deposit is present on all measured profiles whereas the 1997

254   deposit is missing on six (Table 3, Fig. 6). Only on profiles where the sediment limit was not found (e.g. 100), or

255 where profiles dropped to low elevations at their landward extent (001, 180, 160, 140, 100, 130, 210) were "1923"

256 deposits at similar or lower elevations than 1997, and in many of these cases (001, 180, 160, 130), inundation

257 distances for "1923" were longer. Even in the few cases where our field locations did not distinguish 1997 from

258 "1923" by sediment runup or inundation (e.g., Storozh 140, Fig. 9), the "1923" deposit was coarser and/or thicker

259 than 1997.

260

261 **4.3 Chile 1960 deposit**

262 Between "1923" and 1997 deposits on a few profiles (Table 3), there is a thin, patchy and less extensive deposit

263 which we attribute to the 1960 Chile tsunami (e.g., Fig. 4, right). We favor 1960 Chile over 1952 Kamchatka for two

264 reasons. First, the 1960 tsunami was larger than 1952 *in the Kamchatsky Bay region* (Table 1); the more locally

265 generated 1952 tsunami dies off in amplitude along strike of the rupture (MacInnes et al., 2010), whereas the

266 Chilean tsunami on Kamchatka is little affected by latitude (Zayakin and Luchinina, 1987). Second, supporting the

267 1960 interpretation, in one excavation on profile 001, this intermediate tsunami deposit lies above the Bezymianny

268 1955 tephra layer (Fig. 7).

269

270 **4.4 Historical tsunami deposit close below KS$_{1907}$**

271 In many excavations (e.g., profile 100 in Fig. 4, Profile 110 in Fig. 8), there is a tsunami deposit within a few cm of

272 the base of KS$_{1907}$ and which is comparable to 1997 and 1923 in thickness and extent. Although pre-1907

273 sedimentation rates are difficult to determine this tsunami deposit must fall within the historical period, which

274 extends back to 1737. However, the more complete historical records are from southern Kamchatka, and records

275 from the second half of the 19th century are particularly spotty (Gusev and Shumilina, 2004). Thus there is no known

276 historical event we can assign to this deposit; OSL dating might help in interpreting this deposit.

277

278 **5 Discussion – 1997 and "1923" Deposits**

279 **5.1 1997 tsunami**

280 Our observations are consistent with 1997 being a seismogenic tsunami source *with significant rupture energy*

281 *expended in the northern portion of the zone of aftershocks*. The extensive and relatively smooth distribution of

282 runup (Table 3; Fig. 6) and the ratio of maximum runup to distance over which the tsunami had significant runup

283 (on the order of 10^{-5}) indicate that this tsunami was typical of a seismogenic source rather than a landslide source (cf.

284 Okal and Synolakis, 2004). The far-field tide-gage records (e.g., Hilo, Table 1) are also indicative of a broad rather

285 than a point source. Given that the post-tsunami survey reported runup that did not exceed the beach on the

286 Kronotsky Peninsula and that the deposits we mapped north of the peninsula are from the 1997 tsunami, *any source*

287 *model must explain the low (" water") runup on Kronotsky Peninsula and relatively high ("sediment") runup north*

288 *of this peninsula* (Fig 6). Source-region models by Bürgmann et al. (2001) and Llenos and McGuire (2007), e.g., do

289 not include the northern aftershock area, and such models have been used to interpret Kamchatka subduction-zone

290 behavior (e.g., Song and Simons, 2003; Bürgmann et al., 2005; Llenos and McGuire, 2007; Bassett and Watts, 2015).

291 On the other hand, source regions by Gusev et al. (1998; also Gusev, 2004) and Levina et al. (2013) tend to include

292 the entire aftershock zone, overlapping Feb 1923 in the south but also filling the gap between Feb 1923 and April

293 1923 (Fig. S1), which might not be consistent with the tsunami data. Slavina et al. (2007) interpret the southwestern

294 aftershock activity (Fig. 2) to be on a separate, transverse fault, and Kuzin et al. (2007) interpret the SW portion of

295 the (extended) aftershock region to be a separate stress zone, interpretations more consistent with tsunami data.

296 Zobin and Levina (2001) favor most mainshock energy being generated in the middle zone defined by fewer

297 aftershocks (see Fig. 2), but this region is in shallower water, less conducive to tsunami genesis. A recently

298 published finite-fault model resolves to most slip being under the Kronotsky Peninsula, with most energy release

299 focused in the north (Hayes, 2017; https://earthquake.usgs.gov/earthquakes/eventpage/usp0008btk#finite-fault). As

300 with Sohn's 1998 analysis, Hayes' (2017) model cannot explain the 1997 tsunami runup because the rupture is

301 mostly under the Kronotsky Peninsula. Shifting this pattern of deformation eastward could resolve the discrepancy.

302

303 **5.2 1923 tsunamis**

304 There are reasons to favor either or both the 3 February 1923 and the 13 April 1923 Kamchatka tsunamis as the

305 generator(s) of the deposit above KS_{1907} that we identify as "1923" (e.g., Figs. 7,8,9). Given what is known (Table 1),

306 south-central Kamchatsky Bay is the place most likely to have *comparable* runups from each. Both tsunamis have a

307 record in Hilo, but one is runup and the other tide-gage amplitude. There is no case on Kamchatka of a pair of

308 similarly measured records from the same locality with which to compare the two tsunamis, with the exception of

309 observations that the April tsunami generated more damage at the Tsutsumi fish plant southeast of Ust' Kamchatsk

310 (Table S4). The 3 February tsunami was larger in most catalogued locations (Table S4) but apparently smaller than

311 April 1923 in *north* Kamchatsky Bay. The two 1923 tsunamis both occurred while the ground would have been

312 snow covered so that following snowmelt, it would be nearly impossible to distinguish two different deposits. The

313 source regions of the two 1923 Kamchatka tsunamis have been mapped (Fig. 1) but are not easy to constrain in

314 detail other than that the February earthquake was south of Kronotsky Peninsula and the April earthquake north of it

315 (Fig. 1). The February earthquake has been catalogued as Mw 8.3 - 8.5 (ISC event 911271; NCEI) and the April

316 earthquake as Mw 7.1 - 7.3 (ISC event 911331; NCEI), but the local and far-field tsunami runup for April 1923

317 suggests it may have been significantly larger (Gusev and Shumilina, 2004), based on its tsunami, Gusev suggests

318 Mw 8.2 for the April earthquake. A moment magnitude around 7.8 – 8.0 for the April earthquake would be more

319 consistent with its tide-gage amplitude in Hilo (Fig. S2).

320

321 **6 Tsunami deposits pre-20th century back to KS_1 (~A.D. 300)**

322 Goals in reconstructing paleotsunami history include both scientific and practical objectives. Scientifically, southern

323 Kamchatsky Bay paleotsunamis can help us see patterns of subduction-zone behavior. Are the historical tsunamis

324 (and their generating earthquakes) comparable to events in the past? What is the "typical" event and what are the

325 rupture patterns of the northern Kamchatka subduction zone? Practically, these questions apply also to probabilistic

326 hazard analysis – at what frequencies do tsunamis occur and what is their size-frequency relationship?

327

328 **6.1 Occurrence and Size**

329   For the record and analysis of tsunami deposits below KS_{1907}, for each excavation we count the number of deposits

330   between marker tephra and determine the approximate elevation above sea level and distance from shore of the

331   excavation locale in that time (tephra) interval (Fig. S5) (see Figures 7,8,9 and their captions for more detail on our

332   interpretations). For some layers, an excavation may be their limit and for others not (e.g., Fig. 9). We do not

333   attempt to correlate sand layers from excavation to excavation (or profile to profile), though there are cases where it

334   is possible; the problem with distinguishing Feb 1923 from April 1923 deposits illustrates potential for

335   miscorrelation. The reasons that not all deposits are present in all excavations range from preservation to separation

336   – for example, excavations near the coast will commonly contain amalgamated sand layers (e.g., Bourgeois et al.,

337   2006). For each profile, we count the maximum number of tsunami deposits between tephra, which is our indication

338   of how many tsunami events have occurred

339   In order to summarize paleotsunami sizes, we determine sediment runup--or the highest point seaward,

340   whichever is higher--and sediment inundation for tsunami deposits on each profile. For each tephra interval along

341   each profile, there will be deposits at maximum distances and maximum elevations; the two measures are treated

342   separately because tsunami deposits are not correlated (in fact, high runup is associated with shorter, steeper profiles

343   and long inundation with low-relief profiles). For example, for the historical deposits, two points are plotted (Fig.

344   10) – their point of maximum inundation and their point of maximum runup, which are usually on separate profiles.

345   A few of the paleo-events are comparable to Chile 1960 (Fig. 10), but most are likely from locally

346   generated tsunamis because Chile 1960 was an outsized event, and its deposit is not well represented on the profiles.

347   The 1997 tsunami has dimensions similar to the majority of paleotsunamis as represented by sediment runup of on

348   the order of 5-7 m (Fig. 10). The "1923" deposit, for which we do not know if related to February or April or both,

349   is a "typical largest" event (Fig. 10). Recall that in these field sites there are few excavations at elevations of 10 m or

350   more (Fig. S6), and that these higher elevations are on uplifted profiles, so in this situation we cannot have a record

351   of older paleotsunamis reaching such elevations, simply as an artefact of the profile history (Fig. S5). This issue is

352   present also for paleo- inundation on prograding profiles, but is not such a strong artefact in our dataset. Overall, the

353   number of deposits tends to decrease away from the coast and at higher elevations (density of points on Fig. 10),

354   although there is a lot of scatter in the data, likely due to preservation and identification differences (e.g., Fig. 9).

355

356   **6.2 Recurrence**

357   To determine tsunami recurrence according to size, we consider all tsunami deposits above KS_1 (A.D.

358   ~300) at elevations greater than 5 m (Fig. 11). We only use excavations now at or reconstructed to be more than 5 m

359   above sea level or landward of a beach ridge (reconstructed to be) higher than 5 m to be more confident we are

360   analyzing tsunami deposits, not those of storms or floods, and to eliminate most non-local tsunamis. We did not use

361   intermediate Shiveluch tephra layers between KS_{1907} and KS_1 (Table 2) because their presence is not consistent

362   enough to break down recurrence statistics, and the time intervals are short relative to the number of events, so

363   statistical analysis cannot be supported. The grand total of the maximum number of events (per each interval) is 18

364   deposits, including the historical cases. For each event, we determine a maximum sediment runup, that is, if there

365   are four deposits between two marker tephra on a given profile, we determine the four highest points those deposits

366 reach; e.g., two may reach 8.3 m and the other two only 7.2 m (all four reaching 7.2 m). We use reconstructed

367 distances and elevations for each time interval below KS_{1907}. The maximum elevation is either sediment runup, h, or

368 maximum elevation before sediment runup, H (as in Fig. 5), whichever is higher. Independent of the determined

369 maximum elevation, we determine a maximum sediment inundation for each deposit in each tephra interval.

370   All 18 deposits represent large tsunamis, reaching minimum elevations of 5 m (smaller not considered) and

371 inland distances of 100 m, each factor with a recurrence interval of about 100 years (Fig. 11). Note again that runup

372 and inundation are not paired; high runup commonly occurs on shorter, steeper profiles and long inundation on

373 lower profiles. Tsunamis reaching an elevation of at least 7 m have a recurrence of ~200 years (Fig. 11). The largest

374 reconstructed tsunamis as recorded by tsunami deposits have runup of 10 m or more and occur on average every 425

375 yr. Tsunamis with inundation of 600 m or more occur on average every ~570 yr.

376

377 **7 Discussion and conclusions**

378 **7.1 Historical tsunamis**

379   This work adds to the tsunami catalogue for 1997 Kronotsky and 1960 Chile, but not February or April

380 1923 Kamchatka events because we cannot differentiate the (two) 1923 deposits. The nearfield nature of the 1997

381 Kronotsky tsunami is significantly revised by our report herein of coastal profiles north of the Kronotsky Peninsula,

382 adding substantial data to its catalogue. The 1997 tsunami reached runup heights of more than 9 m, averaging 6 m

383 over about 60 km of coastline. As would be expected, tsunami heights (as indicated by deposits) and inundation

384 distances are influenced by coastal topography, with higher runups on steep profiles and longer inundation on lower-

385 relief profiles. Data catalogues do not commonly provide topographic profiles, yet this information can be critical to

386 understanding a tsunami and potentially its generating source.

387   Based on deposits from 15 profiles and more than one hundred excavations, we conclude that in southern to

388 central Kamchatsky Bay the 1923 tsunami (February or April indeterminate) was larger than the December 1997

389 Kronotsky tsunami, but the summary and tabulated data (Fig. 6, Table 3) are tricky to interpret, with sediment

390 inundation (L) being more indicative of tsunami size than runup (h) or highest point seaward of runup (H) (e.g., see

391 Fig. 5 illustration). On the basis of the total number of profiles exhibiting a deposit, "1923" is more extensive, but its

392 average sediment runup (h) value is lower because the farthest point it reached on a number of profiles is actually

393 lower than the closer-to-shore points for 1997. Moreover, even though "1923" exceeded more of the high beach

394 ridges seaward of the (sediment) runup point (H), the average of those is almost the same as for 1997 (Table 3).

395 Thus the most telling measurements *distinguishing* 1997 from "1923" are sediment inundation distances, with the

396 average for "1923" almost twice that for 1997.

397   The 1952 tsunami deposit in southern Kamchatka (and the northern Kuril Islands) (MacInnes et al., 2010)

398 reaches greater heights and inundation distances along its earthquake rupture zone than any of the historical tsunami

399 deposits along the northern part of the Kamchatka subduction zone (this study; also Pinegina, 2014). While this

400 observation is not surprising given that 1952 was Mw 9.0 and the historical events to the north no larger than about

401 Mw 8.5, the question to address is, Can (does) the northern part of the subduction zone produce Mw 9 events, or

402　does Kronotsky Cape represent a locked or continuously slipping zone that keeps ruptures shorter, as in 1923? For
403　that, we must turn to the prehistoric record.
404
405　**7.2 Implications for the 1997 Kronotsky earthquake rupture and the 1923 events**
406　　　　The sediment runup and inundation data reported here require a reevaluation of rupture source models for
407　the 1997 Kronotsky earthquake; we favor slip focused within the northern half of the aftershock zone shown in
408　Figure 2 (also see Fig. S9). *Models which place most rupture energy to the south of or under the Kronotsky*
409　*Peninsula (Fig. S9; e.g., Bürgmann et al., 2001; Bürgmann et al., 2005; Llenos and McGuire, 2007; Bassett and*
410　*Watts, 2015; Hayes, 2017) are not consistent with the tsunami data.* The tsunami, rather than being unusually small
411　for its generating earthquake's moment magnitude (Sohn, 1998), generated runup averaging 6 m over about 60 km
412　of coastline, and 30 cm amplitude on the Hilo tide gage, requiring a "normal" offshore, subduction-zone rupture.
413　Moreover, some significant portion of that rupture must be under substantial water depth to produce the indicated
414　tsunami in the bay north of Kronotsky Cape, while not generating as much runup on the Cape, or to its south. While
415　part of the rupture could well have been under the Kronotsky Peninsula and the relatively shallow region directly
416　offshore, *deformation in deeper water east and north of the peninsula is needed.*
417　　　　We conclude that a rupture consistent with the mainshock and aftershock locations from Kamchatka's
418　network are more reasonable than more westerly locations, e.g., in the ISC catalogue (Fig. 2, Table S2). This issue is
419　illustrated by the Hayes (2017) inversion, which takes the NEIC hypocentral location (Table S2) to start and, while
420　his inversion results in most slip to the north (Fig. S9) locates that slip under the peninsula, where it cannot generate
421　a tsunami. If this inversion were located based on the Kamchatka network's mapped mainshock, it might explain the
422　1997 tsunami.
423　　　　The northern part of the Kamchatka subduction zone ruptured in two large tsunamigenic events in February
424　1923 and April 1923 (Fig. 1), and our study indicates that a substantial portion of the energy released by the 1997
425　Kronotsky earthquake was generated in a seismic gap between those earthquakes (and a large 24 Feb 1923
426　aftershock; Fig. 1), as originally recognized by Fedotov et al. (1998) and predicted by his group's earlier work. The
427　Kronotsky Peninsula lies landward of the (subducting) Emperor Seamount chain, which has been postulated to
428　generate a locked or slowly slipping zone on the KSZ, a zone characterized by a relatively strong positive gravity
429　anomaly (e.g., Bürgmann et al., 2005, Llenos and McGuire, 2007; Bassett and Watts, 2015) (Fig. S9). The behavior
430　of the subduction zone off/under Kronotsky Peninsula may well keep the northern Kamchatka subduction zone from
431　generating 1952-scale (Mw 9) Kamchatka earthquakes, but the 1997 tsunami is evidence that this segment does
432　rupture.
433
434　**7.3 Paleotsunami results – implications for tectonic studies and hazard analyses**
435　　　　Southern to central Kamchatsky Bay has a relatively short but well-preserved record of paleotsunami
436　deposits which can be calibrated with the historical record. Combined with the record in northern Kamchatsky Bay
437　(Pinegina et al., 2012) (the north-central bay is characterized by cliffs), the pattern of runup and inundation in the
438　prehistoric record for the last 1700 years does not diverge from the 20th century record. Compared with southern

439 Kamchatka, the region where Mw 9-scale events occurred in 1952 and 1737, the northern subduction zone has

440 generated smaller and less extensive tsunamis, in agreement with analyses of Bürgmann et al. (2005) for the modern

441 and Pinegina (2014) for the prehistoric record.

442   A robust, 1700-year-long record may be sufficient to generate a probabilistic hazard analysis that can be

443 used for both local and far-field hazard studies, and not only for tsunami recurrence statistics, but also for recurrence

444 statistics that include tsunami size. Reconstructing paleo- runup and paleo- inundation requires, and is thus limited

445 by, accurate reconstructions of past shoreline locations and past (relative) sea levels. Coastlines with well-

446 established marker tephra can enable such reconstructions, as shown by this study.

447   As are seismologists, paleoseismologists are cautioned to qualify our generalizations by the lessons of the

448 11 March 2011 Tohoku earthquake and tsunami. Characterizing subduction-zone behavior and quantifying its

449 hazards are goals which we will only ever accomplish imperfectly.

450 **Supplement link (will be included by Copernicus**) – see supplemental material

451 **Author contribution –** we contributed equally and together

452 **Competing interests** -- none

References

Ammon, C. J., Kanamori, H. and Lay, T.: A great earthquake doublet and seismic stress transfer cycle in the central
 Kuril islands, Nature 451.7178, 561-565, doi:10.1038/nature06521, 2008.

Balakina, L.M.: The October 4, 1994 Shikotan and December 5, 1997 Kronotsky earthquakes and their strongest
 aftershocks as regular manifestations of the tectonic process in the Kuril-Kamchatka seismogenic zone,
 Izvestiya - Russian Academy of Sciences, Physics of the Solid Earth, 36, 903-918, 2000.

Bassett, D. and Watts, A. B.: Gravity anomalies, crustal structure, and seismicity at subduction zones: 1. Seafloor
 roughness and subducting relief, Geochemistry, Geophysics, Geosystems, 16, 1508-1540,
 doi/10.1002/2014GC005684, 2015.

Bourgeois, J.: Geologic effects and records of tsunamis, Chapter 3 in The Sea, volume 15, Tsunamis, Harvard
 University Press, 55-91, 2009.

Bourgeois, J., and Titov, V.V.: A Fresh Look at the 1997 Kronosky Tsunami, Transactions of the European
 Geophysical Society, Abstracts, 2001.

Bourgeois, J., Pinegina, T., Ponomareva, V. and Zaretskaia, N.: Holocene tsunamis in the southwestern Bering Sea,
 Russian Far East, and their tectonic implications, Geological Society of America Bulletin, 118, 449-463,
 doi: 10.1130/B25726.1, 2006.

Braitseva, O.A., Ponomareva, V.V., Sulerzhitsky, L.D., Melekestsev, I.V. and Bailey, J.: Holocene key-marker
 tephra layers in Kamchatka, Russia, Quaternary research, 47, 125-139, doi.org/10.1006/qres.1996.1876, 1997.

Bürgmann, R., Kogan, M.G., Levin, V.E., Scholz, C.H., King, R.W. and Steblov, G.M.: Rapid aseismic moment
 release following the 5 December, 1997 Kronotsky, Kamchatka, earthquake, Geophysical Research Letters, 28,
 1331-1334, doi: 10.1029/2000GL012350, 2001.

Bürgmann, R., Kogan, M.G., Steblov, G.M., Hilley, G., Levin, V.E. and Apel, E.: Interseismic coupling and asperity
 distribution along the Kamchatka subduction zone, Journal of Geophysical Research, 110, B07405,
 doi/10.1029/2005JB003648, 2005.

Fedotov, S.A., Chernyshev, S.D., Matviyenko, Y.D., and Zharinov, N.A.: Prediction of Kronotskoye earthquake of
 December 5, 1997, M = 7.8-7.9, Kamchatka, and its strong aftershocks with M > or = 6, Volcanology and
 Seismology, 6, 3-16, 1998, [in Russian]..

Godzikovskaya, A.A.: Summary of macroseismic information on Kamchatka earthquakes (Pre-instrumental and
 early instrumental observation period), Moscow – Petropavlovsk-Kamchatsky, 134 pp., 2010 [in Russian]..

Gordeev, E.I., Ivanov, B.V. and Vikulin, A.V. (eds.): Kronotskoye earthquake of December 5, 1997 on Kamchatka,
 Petropavlovsk-Kamchatsky, Kamchatkan State Academy of Fishing Marine, 294 pp., 1998, [in Russian with
 English abstracts and figure captions].

Gordeev, E.I., Gusev, A.A., Levin, V.E., Bakhtiarov, V.F., Pavlov, V.M., Chebrov, V.N. and Kasahara, M.:
 Preliminary analysis of deformation of the Eurasia-Pacific-North America plate junction from GPS data,
 Geophysical Journal International, 147, 189-198, doi: https://doi.org/10.1046/j.0956-540x.2001.01515.x, 2001.

502 Gusev, A.A., Levina, V.I., Saltykov, V.A., and Gordeev, E.I.: Large Kronotskoye earthquake of Dec. 5, 1997: basic
503   data, seismicity of the epicentral zone, source mechanism, macroseismic effects, in Gordeev et al., eds., 32-54,
504   1998 [In Russian with English abstract and figure captions].

505 Gusev, A. A.: The schematic map of the source zones of large Kamchatka earthquakes of the instrumental epoch: in
506   Complex seismological and geophysical researches of Kamchatka. To 25th Anniversary of Kamchatkan
507   Experimental & Methodical Seismological Department, Ed. by Gordeev E.I., Chebrov V.N., Petropavlovsk-
508   Kamchatsky, 445 pp., 2004 [in Russian].

509 Gusev, A.A. and Shumilina, L.S.: Recurrence of Kamchatka strong earthquakes on a scale of moment magnitudes,
510   Izvestiya, Physics of the Solid Earth, 40, 206-215, 2004.

511 Hayes, Gavin P.: The finite, kinematic rupture properties of great-sized earthquakes since 1990, Earth and Planetary
512   Science Letters, 468, 94-100, doi: https://doi.org/10.1016/j.epsl.2017.04.003, 2017.

513 ISC, International Seismological Center, On-line Bulletin, http://www.isc.ac.uk, Internatl. Seismol. Cent., Thatcham,
514   United Kingdom, 2014.

515 Kuzin, I.P., Levina, V.I., and Flenov, A.B.: Body wave velocity distribution in the Benioff zone of central
516   Kamchatka during aftershocks of the Kronotskii earthquake of 1997 (M = 7.9), Journal of Volcanology and
517   Seismology, 1, 175-184, doi: 10.1134/S0742046307030037, 2007.

518 Kyle, P. R., Ponomareva, V. V., and Schluep, R. R.: Geochemical characterization of marker tephra layers from
519   major Holocene eruptions, Kamchatka Peninsula, Russia, International Geology Review, 53, 1059-1097,
520   http://dx.doi.org/10.1080/00206810903442162, 2011.

521 Leonov, V.L.: Ground ruptures, landslides and rockfalls caused by the earthquake on December 5, 1997 at the sea-
522   board of Kronotsky Peninsula: in Gordeev et al., eds., 240-246, 1998 [in Russian].

523 Levina, V. I., Lander, A. V., Mityushkina, S. V., and Chebrova, A. Y. The seismicity of the Kamchatka region:
524   1962–2011, Journal of Volcanology and Seismology, 7, 37-57, doi:10.1134/S0742046313010053, 2013.

525 Llenos, A. L., and McGuire, J. J.: Influence of fore‐arc structure on the extent of great subduction zone
526   earthquakes, Journal of Geophysical Research: Solid Earth, 112, B09301, doi:10.1029/2007JB004944, 2007.

527 Liu, P. L. F.: Tsunami modeling: propagation, The Sea, 15, 295-319, 2009.

528 MacInnes, B. T., Pinegina, T. K. Bourgeois, J, Razhigaeva, N, G., Kaistrenko, V. M., and Kravchunovskaya, E. A.:
529   Field survey and geological effects of the 15 November 2006 Kuril tsunami in the middle Kuril Islands:
530   In Tsunami Science Four Years after the 2004 Indian Ocean Tsunami, Birkhäuser Basel, 9-36, doi
531   10.1007/s00024-008-0428-3, 2009.

532 MacInnes, B.T., Weiss, R., Bourgeois, J. and Pinegina, T.K.: Slip distribution of the 1952 Kamchatka great
533   earthquake based on near-field tsunami deposits and historical records, Bulletin of the Seismological Society of
534   America, 100, 1695-1709, doi: 10.1785/0120090376, 2010.

535 MacInnes, B., Kravchunovskaya, E., Pinegina, T., and Bourgeois, J. Paleotsunamis from the central Kuril Islands
536   segment of the Japan-Kuril-Kamchatka subduction zone, Quaternary Research, 86, 54-66,
537   https://doi.org/10.1016/j.yqres.2016.03.005, 2016.

538 Martin, M. E., Weiss, R., Bourgeois, J., Pinegina, T. K, Houston, H. and Titov, V. V. Combining constraints from
539   tsunami modeling and sedimentology to untangle the 1969 Ozernoi and 1971 Kamchatskii tsunamis,
540   Geophysical Research Letters, 35, L01610, doi:10.1029/2007GL032349, 2008.

541 Melekestsev, I.V, Braitseva, O.A., Erlikh, E.N., Shantser, A.E., Chelebaeva, A.I., Lupikina E.G., Egorova, I.A.,
542   Kozhemyaka, N.N.: Kamchatka, Komandor and Kurile Islands, Moscow, Nauka, 439 pp., 1974 [in Russian].

543 Nanayama, F., Furukawa, R., Shigeno, K., Makino, A., Soeda, Y. and Igarashi, Y.: Nine unusually large tsunami
544   deposits from the past 4000 years at Kiritappu marsh along the southern Kuril Trench, Sedimentary
545   Geology, 200, 275-294, https://doi.org/10.1016/j.sedgeo.2007.01.008, 2007.

546 NCEI, National Centers for Environmental Information (formerly NGDC), Natural Hazards Data, Images and
547   Education, Tsunami and Earthquake databases: https://www.ngdc.noaa.gov/hazard/hazards.shtml

548 Okal, E.A. and Synolakis, C.E.: Source discriminants for near-field tsunamis, Geophysical Journal International, 158,
549   899-912, DOI: https://doi.org/10.1111/j.1365-246X.2004.02347.x, 2004.

550 Petukhin, A.G., Dontsov, O.V., Kozlov, V.N., and Sinitsyn, V.I.: Preliminary analysis of strong ground-motion
551   records of the Kronotskoye earthquake of December 5, 1997 (Mw = 7.9): in Gordeev et al., eds., 247-256, 1998,
552   [In Russian with English abstract and figure captions].

553 Pinegina T. K.: Time-space distribution of tsunamigenic earthquakes along the Pacific and Bering coasts of
554   Kamchatka: insight from paleotsunami deposits, Doctor of Geological Science dissertation, Institute of
555   Oceanology RAS, Moscow, 235 pp., 2014 [in Russian].

556 Pinegina, T. K., Kozhurin, A. I., Ponomareva, V. V.: Seismic and tsunami hazard assessment for Ust-Kamchatsk
557   settlement, Kamchatka, based on paleoseismological data, Bulletin of Kamchatka regional association
558   "Educational-scientific center". Earth sciences. 1, 138-159, 2012 [in Russian with English abstract].

559 Pinegina, T.K., Bourgeois, J., Kravchunovskaya, E.A., Lander, A.V., Arcos, M.E., Pedoja, K. and MacInnes, B.T.:
560   A nexus of plate interaction: Vertical deformation of Holocene wave-built terraces on the Kamchatsky
561   Peninsula (Kamchatka, Russia), Geological Society of America Bulletin, 125, 1554-1568,
562   doi: 10.1130/B30793.1, 2013.

563 Ponomareva, V., Portnyagin, M., Pendea, I.F., Zelenin, E., Bourgeois, J., Pinegina, T., and Kozhurin A. A.: A full
564   Holocene tephrochronology for the Kamchatsky Peninsula region: applications from Kamchatka to North
565   America, Quaternary Science Reviews, https://doi.org/10.1016/j.quascirev.2017.04.031 168, 101-122, 2017 .

566 Slavina, L.B., Pivovarova, N.B. and Levina, V.I.: A study in the velocity structure of December 5, 1997, Mw = 7.8
567   Kronotskii rupture zone, Kamchatka, Journal of Volcanology and Seismology, 1, 254-262,
568   doi:10.1134/S0742046307040045, 2007.

569 Sohn, S.W.: The 1997 Kamchatka earthquake. Individual Studies by Participants at the International Institute of
570   Seismology and Earthquake Engineering, Tokyo, International, 34, 91-99, 1998.

571 Song, T. R. A. and Simons, M.: Large trench-parallel gravity variations predict seismogenic behavior in subduction
572   zones, Science, 301, 630-633, doi: 10.1126/science.1085557, 2003.

573 Troshin, A.N. and Diaghilev, G.A.: The Ust' Kamchatsk earthquake of April 13, 1923 , Library Institute Physics
574   Earth, Akad. Nauk SSSR, Moskva, 1926 [in Russian].

575   Zayakin, Yu. A. and Luchinina, A.A.: Catalogue tsunamis on Kamchatka, Obninsk: Vniigmi-Mtsd, 51pp., 1987,
576   [Booklet in Russian].
577   Zayakin, Yu. A. and Pinegina, T.K.: Tsunami in Kamchatka on December 5, 1997: in Gordeev et al., eds., 257-263,
578   1998, [In Russian with English abstract and figure captions].
579   Zobin, V.M. and Levina, V.I.: The rupture process of the Mw 7.8 Cape Kronotsky, Kamchatka, earthquake of 5
580   December 1997 and its relationship to foreshocks and aftershocks, Bulletin of the Seismological Society of
581   America, 91, 1619-1628, doi: 10.1785/0119990116, 2001.

Table 1. 20th century tsunamis affecting the Kamchatsky Bay region of Kamchatka*

Earthquake Parameters			Records of Tsunami Runup (meters) (*tide gage records in italics*) (blank where no record)									
			Locations South to North (see Figure 1)									
Date (local)	Source region	Mw	Kron Bay	Kron. Cape	**Chazhma - Adr-Bistr R.**	3rd River ~45 km s.of U-K	1st River ~30 km s.of U-K	Tsutsumi ~20 km s.of U-K	*U-K tide gage*	Dembi Spit, U-K	Bering I. (south)	Hilo, HI
5 Dec 1997	**Kronotsky Peninsula**	**7.8/7.9^**	**0.5-1**	**1.5**	**this paper**				*gage broken*		*incompl record*	*0.24*
15 Dec 1971	Commander Is.	7.8^							*0.47*			*0.10*
23 Nov 1969	Bering Sea	7.7							*0.2*			*0.10*
24 May 1960	**Chile**	**9.5**	**4**				**3**		*0.8*	**3-4**	**3-3.5**	**~10**
5 Nov 1952	**s. Kamchatka**	**9**	**10-13**			**0.5-1**			*0.1*		**2**	*1.1*
13 Apr 1923	**Kamchatsky Bay**	**7.3/8.2^**					**20#**	**>5**		**11#**	**4**	*0.30*
3 Feb 1923	**Kronotsky Bay**	**8.5^**	**6-8**		**~3 km up Chazhma**			**~3**				**6.10**

*Bold: tsunamis most likely to leave a sedimentary record in south Kamchatsky Bay; see Table S1 for a more complete list of tsunamis and Table S4 for specifics in 1923 cases. Primary sources: Zayakin and Luchinina, 1987; NCEI historical tsunami database

^Kamchatka Mw's from Gusev and Shumilina, 2004; G&S 8.2 for 13Apr23 is based on tsunami; see text discussion

#The 20-m and 11-m numbers are from higher-relief shorelines than the other measurements

582

Table 2. Marker tephra layers <2000 years old in shoreline profile sections, southern Kamchatsky Bay*

Code Field/Classic[^]	Code New*	Source volcano	Modeled age* (years B.P.)	Assigned age* (calendar years)	Field description	Field thickness
KSht$_3$[^]	KSht$_3$	Ksudach	Historical	A.D. 1907	Light to medium gray, fine to very fine sand	0.5-2 cm
SH$_2$	SH#6	Shiveluch	817 +59/-57	A.D. 1134	White (faint gray, yellow white), fs-vfs, has pumice	0.5-1 cm; distinct toward north
SH$_{1450}$	SH#12	Shiveluch	1356 +52/-45	A.D. 596	Pale yellow, yellow gray, lt gray, vfs-ms, salt & pepper —grainy	1-2.5 cm; typically 1-2 cm
KS$_1$	KS$_1$	Ksudach	1651 +54/-61	A.D. 298	Lt brown, beige, "coffee cream"; thin gray cap; si-vfs	1-3 cm; usually not >2 cm

*Ponomareva et al., 2017

[^]Braitseva et al., 1997; in our text, we supplant KSht$_3$ with KS$_{1907}$

583
584

Table 3. Sediment runup and sediment inundation for historical tsunamis above KS_{1907}, southern - central Kamchatsky Bay

Region	Profile #	Latitude	Longitude	1997			1960			1923		
				h	L	H	h	L	H	h	L	H
Bistraya River	001	55.6226	161.7799	3.4	200	5.3	3.3	**126**	5.3	2.0	250	5.3
	001 via river									0	**650**	*
Bistraya River	002	55.59735	161.7680							4.4	205	6.2
	002 via river									2.2	560	*
Bistraya River	003	55.5781	161.7600							4.8	211	6.5
Adrianovka R.	180	55.5275	161.7484	4.8	118	5.6				3.5	367	5.6
Storozh River	150	55.4851	161.7414							2	645	7.7
Storozh River	160	55.4582	161.7394	6.6	159	7.5	**6.2**	107	7.5	6.1	419	7.5
Storozh River	140	55.4387	161.7393	5.8	**330**	5.8				5.8	330	5.8
Storozh River	170	55.3860	161.7340							3.6	267	6.7
Little Chazhma R.	100	55.1407	161.8281	7.4	125	7.4	4.5	107	6.2	7.4	125	7.4
Little Chazhma R.	130	55.1235	161.8379	4.4	109	6.3	4.4	78	5.1	1.8	158	6.3
Chazhma	110	55.1181	161.8408	6.6	200	8.3				8.1	315	8.3
Chazhma	120	55.1019	161.8514	**9.5**	200	9.5				**12**	380	9.5
Big Chazhma R.	220	55.0794	161.8679							7.7	335	9.8
Big Chazhma R.	210	55.0710	161.8760	6.0	305	8.0				6	305	8
Big Chazhma R.	200	55.0629	161.8879							6.6	361	9.1
	200 via river									5	428	*
			AVERAGES	*6.1*	*194*	*7.1*	*4.6*	*105*	*6.0*	*4.9*	*346*	*7.3*

h - elevation of excavation meters above sea level high tide (m a.s.l.); equals "sediment runup" (maxima in bold)

L - distance from the shoreline, m; equals "sediment inundation" (maxima in bold)

H - highest elevation (m a.s.l.), between shoreline and excavation; likely exceeded where there is a sand deposit (max. in bold)

585   *If the tsunami reached a low inland point via the river (indeterminate), H from the profile is not relevant.

586 [Bourgeois & Pinegina FIGURE CAPTIONS]
587
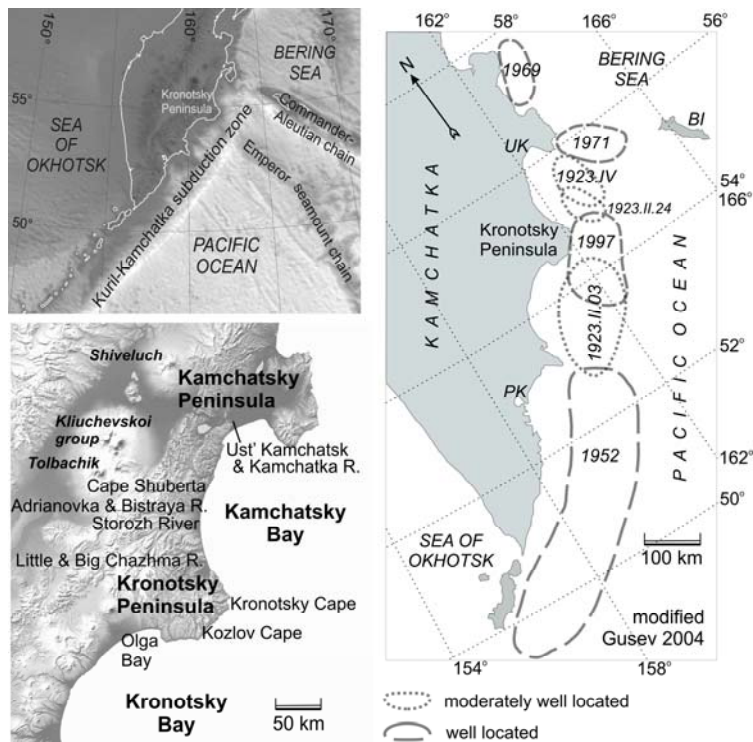
588
589
590 **Figure 1.** General tectonic setting and study locations. **Upper left**: Major topography of and bathymetric features
591 around Kamchatka. **Lower left**: locations of sites mentioned in text and tables. **Right**: Interpreted rupture locations
592 of 20th century tsunamigenic (except *1923.II.24*) earthquakes along the Kamchatka portion of the Kuril-Kamchatka
593 subduction zone (modified from Gusev , 2004, Fig. S1; Martin et al., 2008). The rupture area of the 1997 earthquake
594 shown here is from Gusev (2004) and outlines the entire aftershock zone (Fig. 2). Tide-gage locations PK =
595 Petropavlovsk-Kamchatsky; UK = Ust' Kamchatsk; BI = Bering Island.
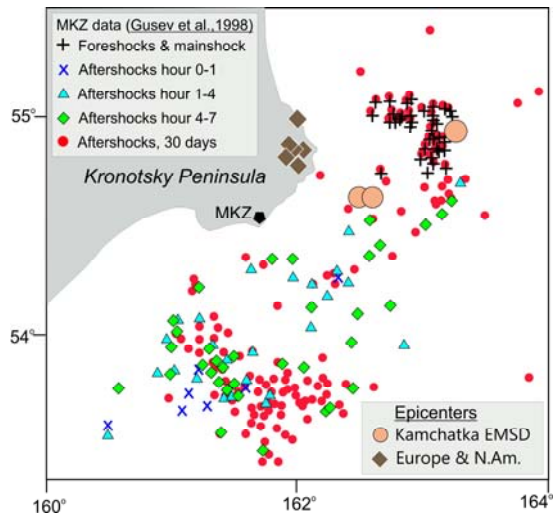
596
597
598 **Figure 2.** Foreshocks (3-5 Dec 1997), mainshock and aftershocks of the 5 December 1997 Kronotsky earthquake
599 (Gusev et al., 1998), including location of nearest seismic station, MKZ. Plotted foreshocks and MKZ aftershocks
600 include only cases where P and S arrivals could be read from MKZ records. Locations of epicenters are from various
601 analyses, both local and farfield as reported from the International Seismological Center (Table S2). Slavina et al.
602 (2007) interpret the southwestern aftershock activity to be on a separate, transverse fault; Kuzin et al. (2007) also
603 interpret the SW portion of the (extended) aftershock region to be a separate stress zone.
604

605
606 **Figure 3.** Photos taken by T. Pinegina on 9 Dec 1997 near Kronotsky Cape (location on Fig. 1). For additional
607 photo and sketch for context, see Fig. S3. **Above** (helicopter for scale): the tsunami deposited sand on the snow up to
608 about the line of grassy vegetation at the back of the beach (see detail, lower right photo); white zone in foreground
609 is sea foam. **Lower left:** Ice and snow broken up by the tsunami (excerpted from photo in Fig. S3). **Lower right**
610 (compass for scale): detail of tsunami-deposited sand above snow that covered the beach, scraped by hand away
611 from a crack in the snow/ice which is interpreted to have been made during an aftershock.
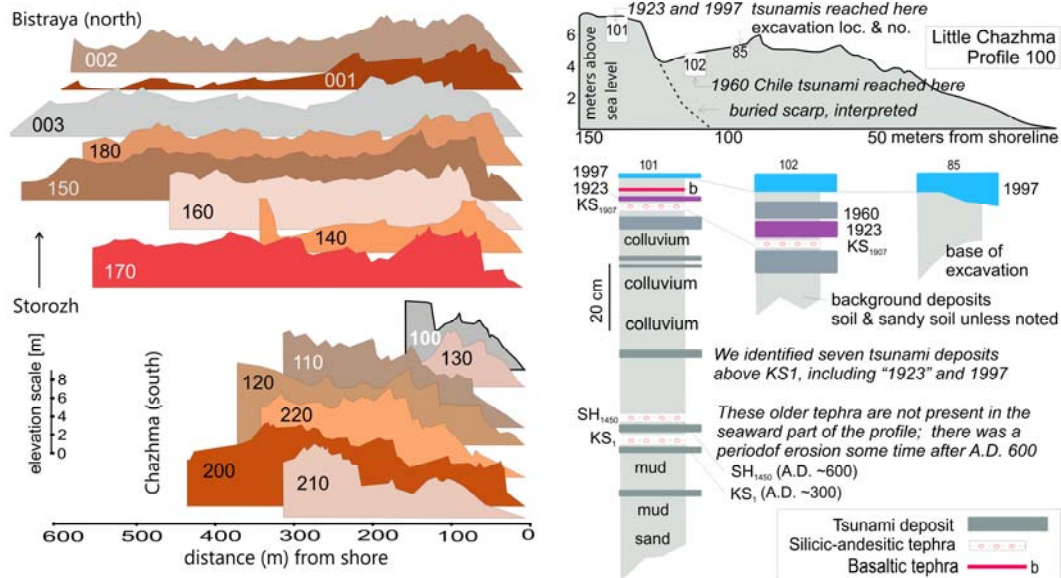
612
613 **Figure 4. Left**. Topographic profiles measured in southern Kamchatsky Bay (locations on Fig. 1, arranged from
614 south (bottom) to north (top), except 001 and 002 reversed to reveal topography. Distances and elevations are
615 measured from 0 at the water line (lower right corner of each profile), corrected to high tide. **Right**: Chazhma
616 Profile 100 used as a key to collected profile data and interpretations *(interpretation in italics)*; background deposits
617 are soil or sandy soil, unless noted.
618
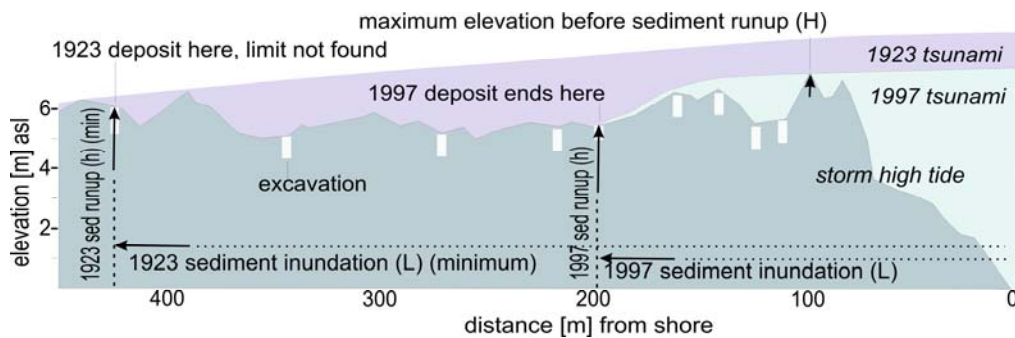
619
620 **Figure 5.** Terminology for sediment runup and sediment inundation, and interpretation of deposits from 1997 and
621 1923, using example of an actual profile (Storozh 160; vertical exaggeration ~10). Near the shoreline on this profile,
622 both tsunamis had to exceed a point (H) higher than "sediment runup" (h) and that, although the minimum sediment
623 runup for 1923 is not much greater than for 1997, 1923 was likely higher to generate greater inundation, which is
624 also be related to tsunami wave length. Note that a 2-D interpretation of (orthogonal) tsunami flow over this and
625 most study profiles is justified by the lateral continuity of ridges. In a few cases (discussed in text), the tsunami may
626 have reached a runup/inundation point via a lower, more circuitous route. Distances and elevations are from
627 surveying.
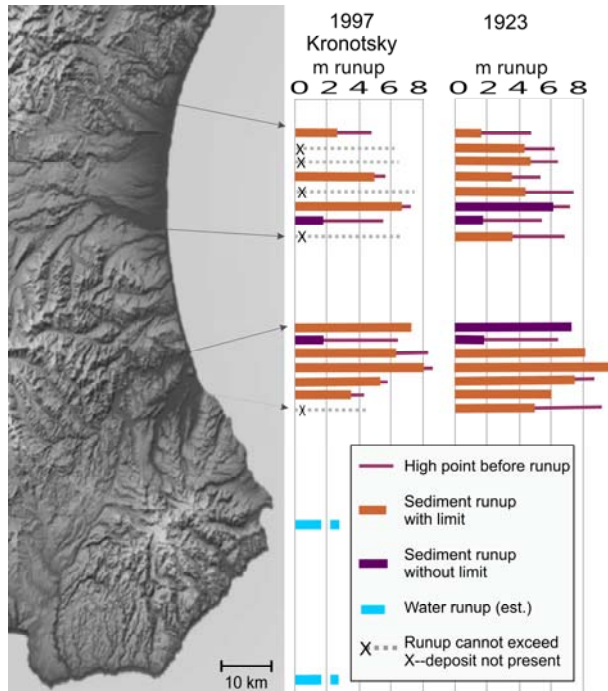
628
629 **Figure 6.** Water runup (Zayakin and Pinegina, 1998) and sediment runup (this paper, Table 3) for the 1997
630 Kronotsky tsunami on and north of the Kronotsky Peninsula, southern Kamchatsky Bay (locations on Figure 1; also
631 see Fig. S2). Water runup was not measured with instruments but was estimated; tsunami did not exceed the
632 unvegetated beach (e.g., Fig. 3); it could have been somewhat higher than reported, shown on this figure by dashed
633 blue line. Sediment runup is also illustrated for the tsunami deposit closely above KS_{1907}, which we interpret as from
634 1923 February or April (see text discussion). Sediment inundation is given in Table 3, as well as latitudes and
635 longitudes for the 15 profiles. Figures 4 and 5 illustrate methods and terminology.
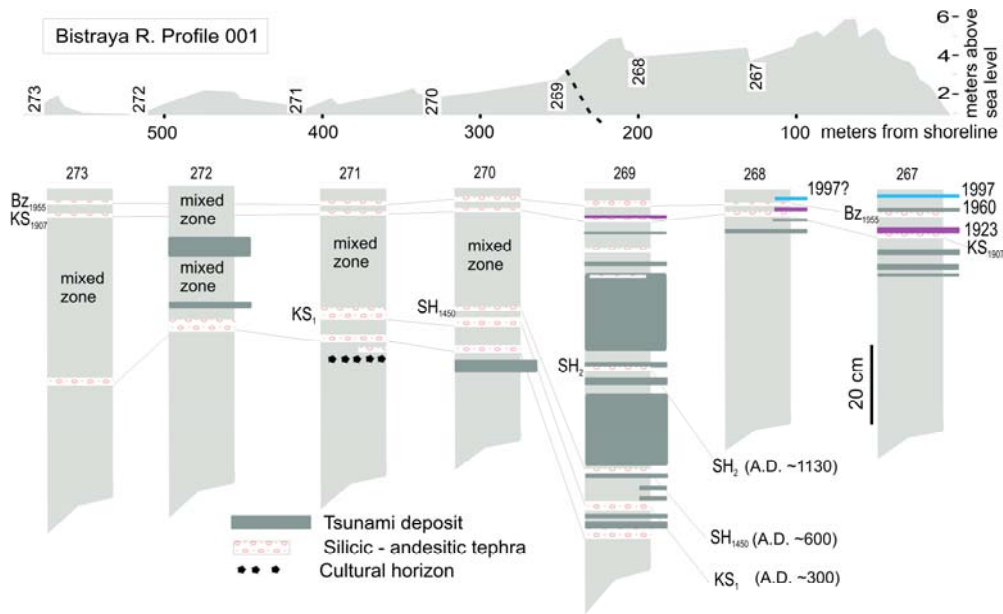
636
637 **Figure 7.** Northernmost profile, southern Kamchatsky Bay (Fig. 1 location; more extensive key in Fig. 4; tephra and
638 tsunami deposits that are shown as narrower bands, e.g., 1997 in excavation 268, indicate thin, patchy deposits).
639 This profile shows evidence of subsidence through time -- the landward part of the profile is lower. This lower
640 profile has been subjected to river erosion -- the "mixed zone" is mostly fluvial sediment containing clasts of older
641 material. Excavations having this mixed zone (273 to 270) all contain a tephra older than KS_1, indicating that older
642 strata are preserved below the reworked material. In this profile 001, there is an ash layer from the 1955 eruption of
643 Bezymianny, a year before its major eruption. With this tephra present, we can assign the tsunami deposit above (in
644 excavation 267) to Chile 1960 rather than to Kamchatka.
645
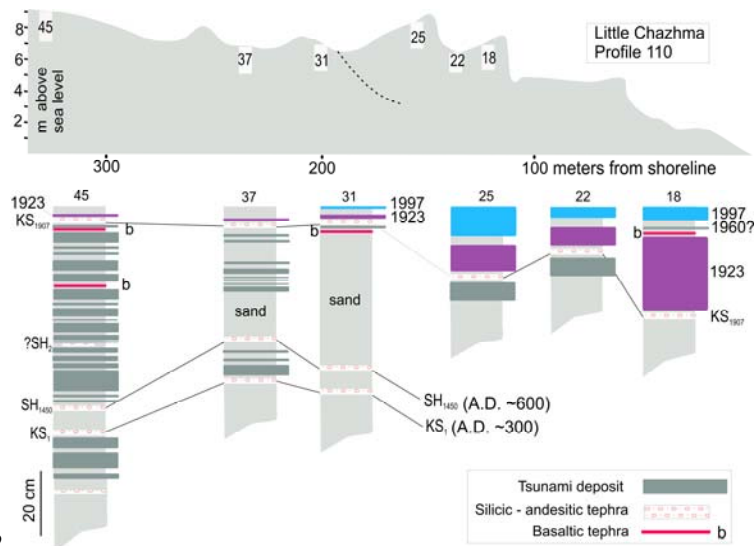
646 1952.
647 **Figure 8.** Profile 110, Chazhma area (Fig. 1 location; more extensive key in Fig. 4). This profile has been uplifted
648 through time – the landward part of the profile is higher. Exc. 45 contains many tsunami sand layers currently at
649 high elevation, which when reconstructed were lower (Fig. S5).In excavations 37 and 31, some of the section was
650 too sandy (not enough soil development) to distinguish individual sand layers. The profile shows the distribution of
651 20th century deposits, as well as a tsunami deposit very close below KS_{1907}. The 1923 tsunami(s) reached the highest
652 point shown on this profile, whereas 1997 and "below KS_{1907}" were smaller. The deposit we tentatively assigned to
653 Chile 1960 on this profile is not included in Table 3 because the deposit was not well preserved; it is higher than any
654 other excavation containing a deposit we attribute to Chile 1960.
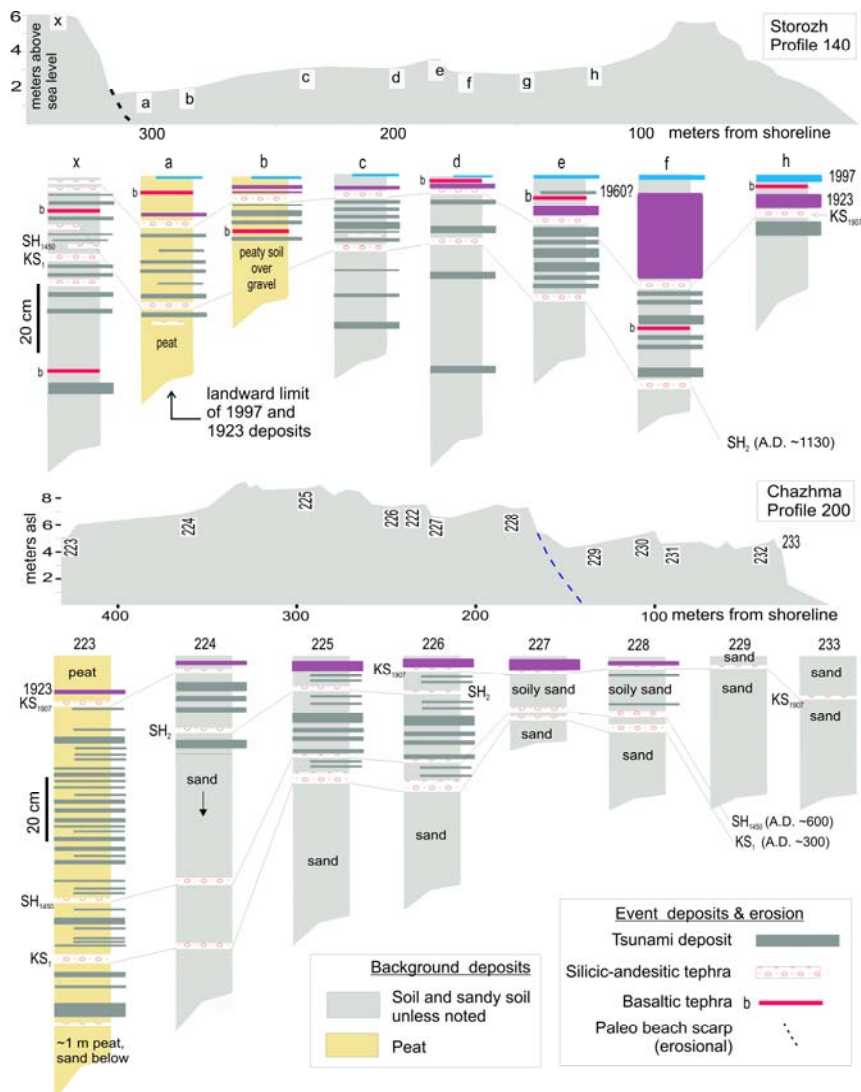
Figure 9. Example of two profiles that illustrate paleotsunami deposits used in analyses. Also see Figs. 4, 7, 8; ; tephra and tsunami deposits that are shown as narrower bands, e.g., 1997 in excavation 268, indicate thin, patchy deposits **Storozh Profile 140 (top)**. Here we use this profile to illustrate an analysis of tsunami deposits between KS_{1907} and SH_2; note that the deposits thin landward, in general. In most excavations there are six tsunami deposits between KS_{1907} and SH_2; excavation "x" has only three. Thus all six tsunamis reached "a" but only three reached "x"; or, three of the six tsunamis only reached "a". All six tsunamis had to exceed the height of the shoreward beach ridge at the time of deposition. **Chazhma Profile 200 (bottom).** As in Profile 110 (Fig. 8) this profile has undergone uplift through time. For sub-SH_2 deposits, the profile was reconstructed to 4 m lower and 150 m narrower. Sites 229-233 are young; the profile from 228 landward is older than KS_1 (A.D. ~300). Site 223 is not far from the modern Chazhma River and in the past some tsunamis may have flooded this site via the river, when the profile was lower. Sites 226 and 225 both have six deposits between SH_2 and SH_{1450}; no other excavation on this profile provides a good count in this interval, but these six deposits probably are in the record at 223, and 224 was simply too sandy (lacking soil separation between layers) to count all layers in this interval. SH_2 is not preserved (was not detected) in the peat excavation (223), but the 23 tsunami deposits in this excavation can be used in the overall count above KS_1. Excavations 223, 225 and 226 all preserve tsunami deposits between SH_{1450} and KS_1. In this interval the peat excavation (223) contains six deposits to the two in 225 and 226, for two possible reasons; first, peat is a better preserver/displayer of thin layers, and second, 223 is lower than 225 and 226 and at this time all were closer to shore. For the latter reason, 223 may have received tsunamis and their deposits directly from the river rather than over the beach ridge(s).
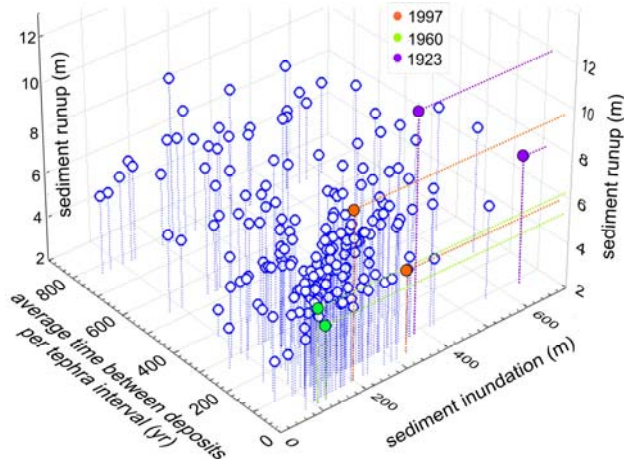
Figure 10. Three-dimensional diagram summarizing sediment runup and inundation for tsunami deposits, south Kamchatsky Bay, above KS$_1$ tephra (A.D. ~300, up through A.D. 2000) (from data plotted in Figs. S7 and S8). The three historical tsunami deposits are highlighted with their two points of maximum runup (and corresponding inundation at that point) and maximum inundation (and corresponding runup at that point), which do not coincide. For prehistoric events, we calculated (sediment) runup and inundation per tephra interval, with adjustments for changes through time in shoreline location and excavation elevation (see text and Fig. S5).
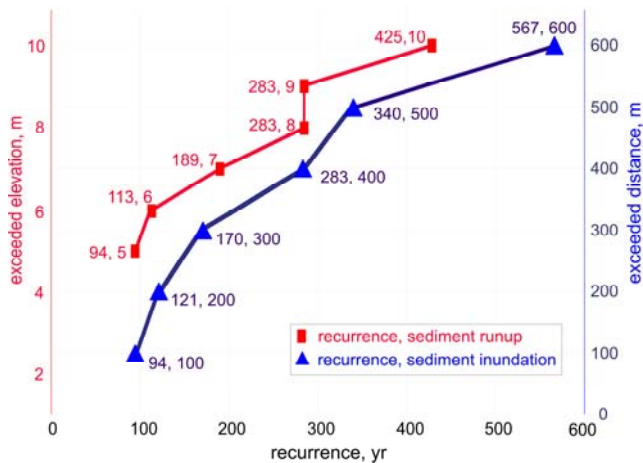
Figure 11. Tsunami (>5 m) recurrence for exceeded elevations (sediment runup) and exceeded distances from shoreline (sediment inundation) based on tsunami deposits since KS$_1$ (A.D. ~300) in south Kamchatsky Bay. (For runup, integers of m are shown; for inundation, multiples of 100 m.) For example, tsunamis with runup of 8-9 m or more occur on average every 283 years. Tsunamis exceeding inundation of 500 m occur on average every 340 years. Recall that runup and inundation are not paired (see text).